JOURNAL OF GEOPHYSICAL RESEARCH, VOL. 97, NO. B3, PAGES 3397–3404, MARCH 10, 1992

The Electrical Conductivity of an Isotropic Olivine Mantle

STEVEN CONSTABLE

Scripps Institution of Oceanography, La Jolla, California

THOMAS J. SHANKLAND

Los Alamos National Laboratory, Los Alamos, New Mexico

AL DUBA

Lawrence Livermore National Laboratory, Livermore, California

In order to extend the useful temperature range of interpretation of olivine electrical conductivity σ we have used the nonlinear iterative Marquardt technique to fit experimental data over the range 720°–1500°C to the parametric form $\sigma = \sigma_1 e^{-A_1/kT} + \sigma_2 e^{-A_2/kT}$, where k is Boltzmann's constant and T is absolute temperature. The model describes conduction by migration of two different thermally activated defect populations with activation energies A_1 and A_2, and preexponential terms σ_1 and σ_2 that depend on number of charge carriers and their mobility and that may be different for each crystallographic direction. A combined interpretation of recent high (San Carlos olivine) and low (Jackson County dunite) temperature measurements has been made that demonstrates that a single activation energy A_1 for all three crystallographic directions adequately fits the data. The parametric fits show that the high-temperature conduction mechanism has far greater anisotropy than the low-temperature mechanism, consistent with previous assignments to ionic and electronic conduction, respectively. The geometric mean of the conductivity in the three directions is approximately $\bar{\sigma} = 10^{2.402} e^{-1.60eV/kT} + 10^{9.17} e^{-4.25eV/kT}$ S/m and is presented as a model for isotropic olivine, SO2, appropriate from 720°C to above 1500°C, at oxygen fugacities near the center of the olivine stability field. It is observed that the magnitudes of σ_1 for the three crystal directions are similar to the ratios of the inter-ionic distances between the M1 magnesium sites in olivine, to within 5%, consistent with Fe^{3+} preferring the M1 site below 1200°C.

INTRODUCTION

Electrical conductivity is one of the few mantle properties that can be sensed from Earth's surface, and laboratory studies of olivine and olivine-rich rocks are extremely important in the interpretation of field and observatory studies of mantle conductivity. Recently, *Shankland and Duba* [1990] presented data for the three principal axes of a single crystal of San Carlos olivine (SCO), between 1200°C and 1500°C. These data were collected as part of a more general study by *Schock et al.* [1989]. The SCO data show an anisotropy of about a factor of 2 for the most resistive and most conductive axes, [010] and [001], respectively. *Shankland and Duba* [1990] used various mixing laws to infer the conductivity of an isotropic, polycrystalline olivine rock from the three axis data; upper and lower bounds, which differ by 15%, were obtained by parallel and series mixing laws. The results from the application of various binary mixing schemes to the series and parallel bounds and the application of the geometric mean to the three axes differ only by 3%. One set of these results, a standard olivine model SO1, related temperature and conductivity over the 1200°–1500°C temperature range of the measurements; at the lower temperatures of the lithospheric mantle, conductivities extrapolated from SO1 are significantly higher than those recently measured on olivine polycrystals. For example, *Constable and Duba* [1990] presented the conductivity of an isotropic, polycrystalline olivine rock (a dunite from Jackson County, North Carolina, or JCD) between 640°C and 1100°C, and *Tyburczy and Roberts* [1990] examined a sintered, polycrystalline San Carlos olivine between 800 and 1300°C (Figure 1).

Although low-temperature extrapolation of SO1 also diverges from earlier data for the [010] direction of Red Sea peridot (or RSP, Figure 1 [*Duba et al.*, 1974]), the SCO data of *Shankland and Duba* [1990] are more applicable to mantle conditions in their temperature range than any other current data set. SCO is a mantle olivine, unlike JCD and RSP which are metamorphic in origin and systematically of lower conductivity, and the experiments were done with as little modification or alteration of the sample as possible. Data above 1200°C cannot be collected at atmospheric pressures from lherzolites without melting of samples. The SCO data are also complete in that they are available for all three principal axes. However, with the exception of sparse data in the [100] direction (Figure 1), there are no three-axis low-temperature data for SCO currently available.

The purpose of this paper is to combine the high-temperature, anisotropic SCO data with activation energies inferred from the lower-temperature data in order to provide a single $\sigma - T$ curve appropriate for an extended temperature range in the mantle. We also make improvements in the methodology used to fit the standard olivine model to the SCO data and introduce some preliminary data from a mantle lherzolite in support of our model.

EXPERIMENTAL METHOD AND CONDUCTIVITY DATA

An understanding of the experimental method and f_{O_2} dependences in olivine are important in understanding the limitations of the parameter fitting and our treatment of the various data sets. All the measurements discussed in this paper were collected using a furnace in which f_{O_2} is controlled by pass-

Paper number 91JB02453.
0148-0227/92/91JB-02453$05.00

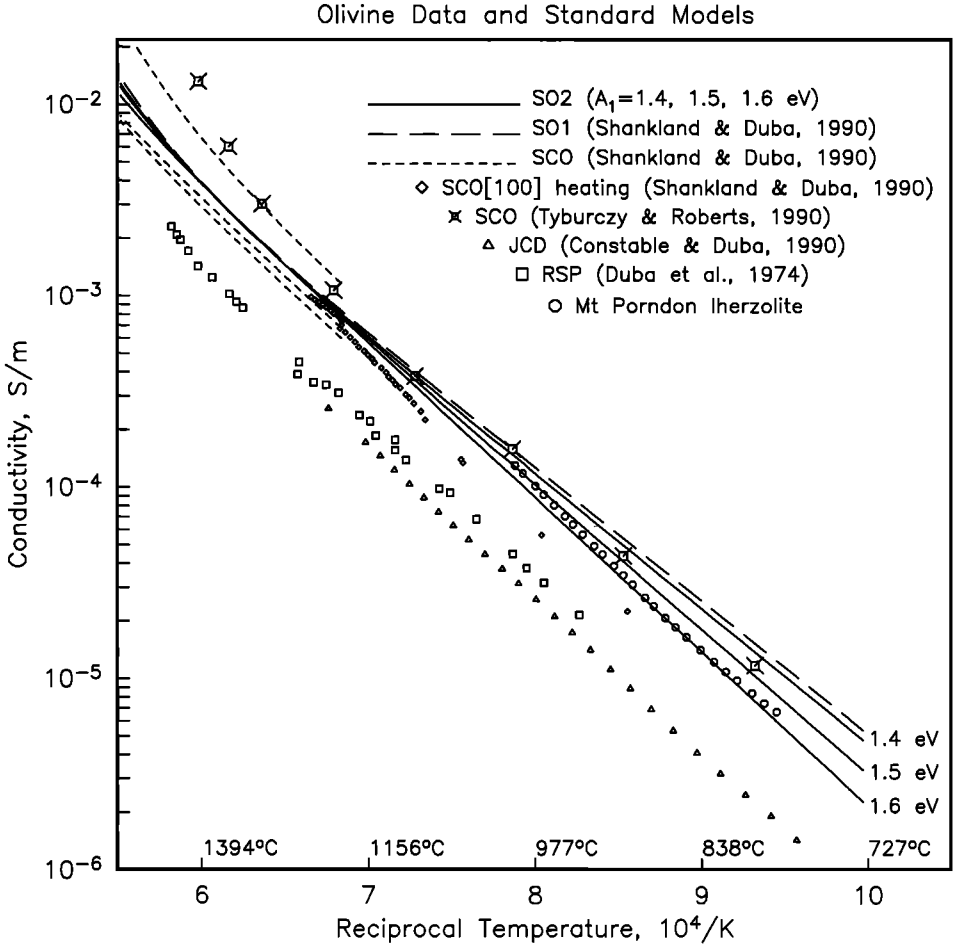

Fig. 1. Conductivity versus temperature for various olivine samples and fits. The higher-temperature SCO data (three short dashed lines) are represented by the fits shown in Figure 2. The lower-temperature single crystal data for Red Sea peridot [010] (squares, [*Duba et al.*,1974]) and SCO [010] (diamonds) are shown. Jackson County dunite (triangles) is represented by every second datum from *Constable and Duba* [1990], and a lherzolite (circles) is represented by every fourth datum from the original experiment (A. Duba and S. Constable, work in progress, 1991). Stars are grain interior conduction estimates for crushed and sintered SCO [*Tyburczy and Roberts*, 1990]. The similarity in activation energies for all data below 1200°C strongly suggests that a single activation energy is sufficent to describe all three crystallographic axes. It is notable that the metamorphic olivines (JCD and RSP) are significantly less conductive than the mantle olivines SCO and the lherzolite and that all measurements made on mantle materials group into a relatively tight band with less than 1/3 decade dispersion below 1200°C. *Shankland and Duba*'s [1990] SO1 model is shown (long dashed line), as well as SO2 for the low temperature activation energy fixed at 1.4, 1.5, and 1.6 eV (solid lines). We see that for 1.4 eV, SO2 is comparable to SO1 but that SO2 for 1.6 eV provides a much better match to the activation energies of the lower temperature data.

ing a mix of CO and CO_2 at atmospheric pressure across the sample [*Duba et al.*, 1990; *Tyburczy and Roberts*, 1990]. Control of oxygen activity is necessary to maintain olivine within its stability field and because olivine exhibits a dependence of conductivity on f_{O_2}. A fixed gas ratio is normally used, which has the advantage that f_{O_2} increases with temperature subparallel to the the boundaries of the olivine stability field and follows the quartz-fayalite-magnetite (QFM) or wustite-magnetite buffers. The disadvantage of using a fixed gas mix is that the activation energies estimated from the data, while applicable to parametric models of mantle conductivity, are a little different from the activation energies of the solid-state processes responsible for conduction because of the f_{O_2} dependence of conductivity. Most measurements were made using a gas mix which generates an oxygen partial pressure of 10^{-4} Pa at 1200°C; close to the QFM buffer. However, because f_{O_2} varies with temperature for a fixed gas mix, during heating or cooling there is a continuous lack of equilibration with the experimental gas mix. This effect can be seen in the jump in the conductivity of San Carlos [100] in Figure 1 at 1200°C, where there is a pause in the heating rate to allow the sample to come to equilibrium. There is a similar jump in the [010] data (the [001] data were collected during cooling with no pause). *Constable and Duba* [1990] quantified this lack of equilibration and showed that the maximum error should be $\theta A \tau$, where θ is the heating rate, A is the increase in conductivity per degree increase in temperature due only to the change in f_{O_2}, and τ is the characteristic time for reequilibration after a change in f_{O_2}. For SCO, $\theta A \tau$ is approximately 1 C°/min$\times$ 0.0017 $\log_{10}(\sigma)$/C°$\times$ 25 min = 0.042 $\log_{10}(\sigma)$. Comparison with the magnitude of the jumps indicates that this is a rea-with the magnitude of the jumps indicates that this is a reasonable estimate.

For the purposes of estimating activation energy by param-

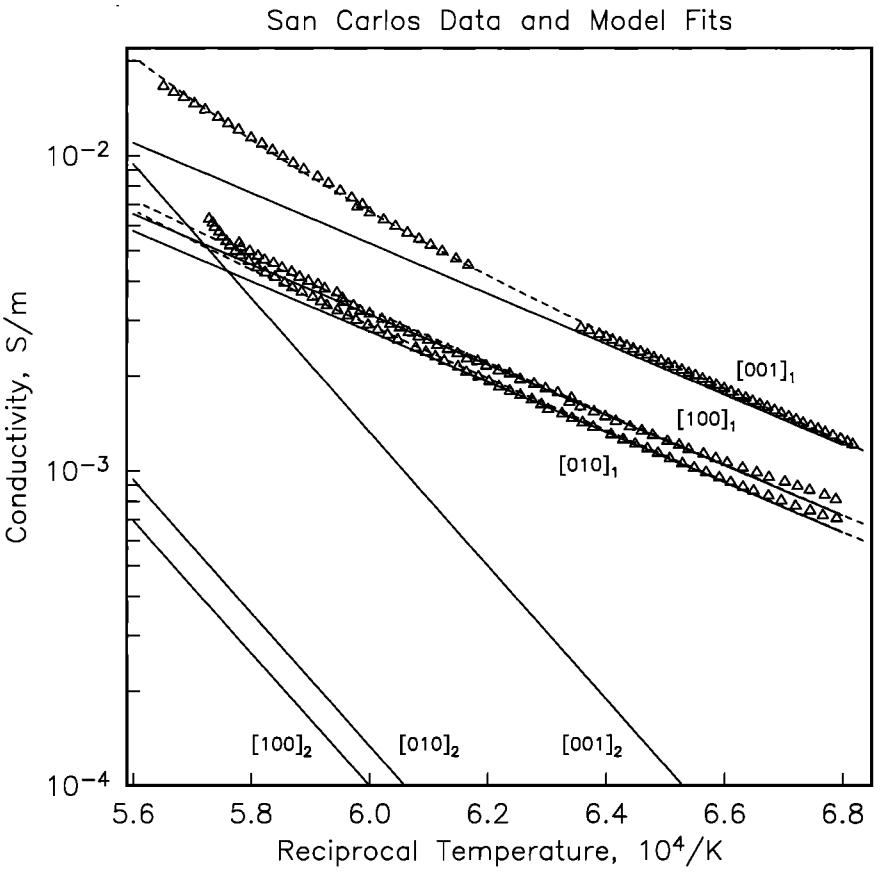

Fig. 2. Conductivity versus temperature for the three crystallographic directions of San Carlos olivine (triangles, data from *Shankland and Duba*, [1990]). The dashed lines are the fits according to the parameters of Table 2 with a low-temperature activation energy of 1.6 eV. The 10 highest temperature data in the [010] direction have been excluded from the fitting. The solid lines show the fits decomposed into high- (subscript 2) and low- (subscript 1) temperature components for the three directions. It is clear that conduction is dominated by the low-temperature component and that anisotropy is greater for the high-temperature component.

eter fitting, it is better to have a constant heating rate and therefore (at least over a limited temperature range) a constant lack of equilibration, than to have the systematic changes in slope that results from changes in heating rate. The effect is only small (0.04 decade), and will be accommodated without elimination of data by fixing A_1 a priori, but is probably responsible for the low activation energy estimated for [100] by *Shankland and Duba* [1990].

Another systematic effect that is expected to bias the parameter fitting is the unusually rapid change in slope in data for the [010] direction above 1450°C (Figure 2). The model given in equation (1) produces a poor fit to these data, and yields an activation energy greater than the band gap [*Shankland and Duba*, 1990]. Given the ease with which the sample can be metamorphosed at high temperatures we speculate that the sudden change in slope is anomalous and results from alteration, perhaps from a furnace contaminant during this run. Although upon examination the sample does not appear to be melted or oxidized, our speculation is supported by the (unpublished) cooling data for this run, which follow a path that is much more conductive and has a lower activation energy than the heating data. If this alteration were an actual property of San Carlos olivine, we would expect all three directions to show the effect. We have consequently removed the 10 highest-temperature data in the [010] direction from the analysis. Shankland and Duba retained these data because their aim was to fit the data as they were for the purpose of the spatial averaging, on which they had little effect.

None of the materials discussed so far are mantle rocks; they are single crystals, a synthetic polycrystal, and a natural metamorphic polycrystal. Effort is underway to extend the measurements to mantle polycrystals, and preliminary data from a lherzolite collected from Mount Porndon, Australia (A. Duba and S. Constable, manuscript in preparation, 1991) are presented here in Figure 1. The lherzolite is approximately 60% olivine, 35% pyroxene, and 5% spinel, and the conductivity measurements were collected at the same f_{O_2} as the SCO measurements made by *Schock et al.* [1989]. Unlike JCD, this material contains mantle olivine of similar iron content to SCO and so may be compared more directly with the data we wish to analyze. Although the conductivity of this rock appears to be dominated by olivine, because of pyroxene and minor minerals the chemical environment of that olivine is much more complicated than of the single crystal measurements, and the activation energy is about 1.9 eV, which is larger than for the other low-temperature data sets we have been considering. The data are preliminary in that we have not yet analyzed σ as a function of f_{O_2} or examined higher-temperature behaviour. However, the dominant feature of all the data involving the mantle materials San Carlos olivine and

Mount Porndon lherzolite is their narrow band of variation under all circumstances of study. This agreement strengthens the hypothesis that a useful relationship between temperature and conductivity can be derived for mantle materials based on laboratory studies.

PARAMETRIC FITS TO OLIVINE CONDUCTIVITY DATA

Both data and theory for conduction in minerals support the use of an Arrhenius relationship between conductivity and temperature, which for two conduction mechanisms with activation energies A_1 and A_2 is

$$\sigma = \sigma_1 e^{-A_1/kT} + \sigma_2 e^{-A_2/kT} \quad (1)$$

where k is Boltzmann's constant and T is absolute temperature. *Constable and Duba* [1990] demonstrated the use of the non-linear, least squares parameter estimation method of *Marquardt* [1963] to recover the coefficients $\sigma_{1,2}$ and activation energies $A_{1,2}$ from a set of conductivity–temperature data. *Shankland and Duba* [1990] applied this method to conductivity data measured along each axis of SCO and also to one of the binary averaging schemes to obtain coefficients and activation energies for an isotropic olivine rock. They adopted the general model in which the activation energies $A_{1,2}$ for the different axes were different and independent; after spatial averaging the six activation energies were reduced to two. When the polycrystal data are considered, it becomes clear that this fitting can be revised and simplified, for the following reasons.

First, the low-temperature activation energies modeled for SCO (0.97–1.52 eV) are significantly lower than the activation energies of the polycrystals (Table 1), which are 1.49, 1.60, and 1.92 eV. When the SCO fits are extrapolated to 700°C, there is up to an order of magnitude mismatch between the SCO conductivities and those of the polycrystals.

Second, data from the polycrystals exhibit extremely little curvature on an Arrhenius plot between 700° and 1200°C, implying that any variation in activation energy between axes is too small to be measured. For the data of *Constable and Duba* [1990] one activation energy of 1.60 eV is maintained over 480 C° (Figure 1). Furthermore, the only low-temperature data available for the SCO experiments, collected on heating a SCO [100] sample from room temperature [*Shankland and Duba*, 1990], also have an activation energy close to 1.6 eV (Figure 1), rather than the 1.11 eV obtained using the high temperature data alone. (Unfortunately, heating data for the other two axes are not available.) *Tyburczy and Roberts* [1990] obtained 1.49 eV for grain interior conductivity in a sintered, polycrystalline SCO; this result agrees well with JCD, especially after considering the different sample preparation (sintering) and the different origin of the olivine.

Third, it is well known that in fitting exponentials there can be a great deal of correlation between the preexponential terms and the activation energies. This is particularly true if the fitting is done over a relatively limited temperature range, as by Shankland and Duba. This explains why A_1 can be essentially the same for the three axes and still be consistent with Shankland and Duba's data over a limited temperature range. The errors in Table 1 were derived from the diagonal elements of the parameter covariance matrix, but in many cases the off-diagonal terms will also be large. The parameter correlation matrix illustrates this problem. If c_{ij} are the elements of the covariance matrix, the symmetric matrix of linear correlation coefficients is given by

$$cor_{ij} = \sqrt{\frac{c_{ij}^2}{c_{ii}c_{jj}}}.$$

For example, the fit of (1) to the [010] data of San Carlos olivine has the correlation matrix

	$\log_{10}(\sigma_1)$	A_1	$\log_{10}(\sigma_2)$	A_2
$\log_{10}(\sigma_1)$	1.000			
A_1	1.000	1.000		
$\log_{10}(\sigma_2)$	0.788	0.779	1.000	
A_2	0.792	0.783	1.000	1.000

We see that σ_1 is highly correlated with A_1 and σ_2 is highly correlated with A_2. This means that an increase in activation energy can be offset by an increase in the corresponding coefficient, a trade-off that is not reflected when selecting errors from the diagonal elements of the covariance matrix, which makes the implicit assumption that the parameters are independent. Covariance is not a problem for a purely parametric description of the data, as used by Shankland and Duba, but is a problem if an interpretation is placed on the A_i and σ_i, or if an extrapolation is required. Quantitative interpretation of the correlation coefficients is difficult. Normally, one would test the coefficients against the maximum value one would get from an uncorrelated population, say, 95% of the time. This depends on the number of degrees of freedom, which for this example appears to be 63 data - 4 parameters = 59, implying

TABLE 1 Fits to Activation Energy Between 700° and 1500°C

Material and Reference	A_1, eV	f_{O_2}, Pa	Fe/(Fe+Mg)	Temperature, C
San Carlos olivine (*Shankland and Duba*, 1990]				
[100]	1.11 ± 0.10	10^{-4}	0.087	1200–1500
[010]	1.52 ± 0.02	10^{-4}	0.087	1200–1500
[001]	0.97 ± 0.11	10^{-4}	0.087	1200–1500
SO1	1.38 ± 0.04	10^{-4}	0.087	1200–1500
San Carlos olivine [100] heating (this paper)	1.66 ± 0.01	10^{-4}	0.087	900–1500
Jackson County dunite [*Constable and Duba*, 1990]	1.60 ± 0.01	$10^{-4.5}$	0.073	650–1200
Red Sea peridot (fit from *Constable and Duba* [1990])	1.53 ± 0.02	10^{-3}	0.096	900–1450
Sintered SCO [*Tyburczy and Roberts*, 1990]	1.49 ± 0.04	10^{-5}	0.09	800–1400
Lherzolite (A. Duba and S. Constable, manuscript in preparation, 1991)	1.92 ± 0.01	10^{-4}	0.09	605–1010

Low-temperature activation energies for various olivines. f_{O_2} refers to oxygen fugacity at 1200°C.

that 95% of the time the correlation coefficient would be 0.254 or less in uncorrelated series [*Bevington*, 1969]. However, if one examines the residuals (data minus the model predictions) versus T^{-1}, one finds that the sign of the residuals form only five runs (a run is an unbroken sequence of residuals with one sign), indicating the data are not independent of each other (see a description of the runs test given by *Crow et al.* [1960, pp. 83–85]) and that the number of degrees of freedom is much smaller than 59. The reduction in degrees of freedom arises from the close sampling of the data in time and temperature, and the systematic departures from equilibrium discussed above. For 6 degrees of freedom the 95% level would be 0.811.

Another approach to examining parameter independence is to perform a singular value decomposition of the linearized system [*Lanczos*, 1960] (for a geophysical application, see *Jupp and Vozoff* [1975]). From this we learn that the resolved parameter eigenvectors, or orthogonal linear combinations of physical parameters, are approximately $0.95A_1 - 0.30\log_{10}(\sigma_1)$, $0.94A_2 + 0.32\log_{10}(\sigma_2)$ and $0.29A_1 + 0.95\log_{10}(\sigma_1)$. While it is clear that significant correlation between A_1 and σ_1 exists, it is probably not as bad as the correlation coefficient of 0.9996 implies because the first and third eigenparameters are dominated by A_1 and σ_1. Finally, one must caution that the above considerations only hold in the linear approximation, while the true problem is nonlinear.

Considering the evidence from the polycrystal data that the activation energies A_1 are essentially the same in all three directions and having justified trading off variations in A_i with variations in σ_i during the parametric fitting, we will consider the less general case of a single pair of high- and low-temperature activation energies, A_1 and A_2, for all three axes. We use a fixed A_1 obtained from polycrystal data collected at lower temperature. We can impose a low-temperature activation energy on the SCO data because the limited temperature range of the SCO data provides ability to trade off A_1 and σ_1. We include only the slope from the lower-temperature data directly in the parameter estimation because variations in sample preparation, sample origin, iron content, and f_{O_2} will all alter σ_1 [*Schock et al.*, 1989; *Constable and Duba*, 1990]. Thus the low-temperature intercepts σ_1 are determined by the lower-temperature portions of SCO, and the new fit will lie above JCD and parallel to it. A dependence of A_1 on f_{O_2} and iron content might be expected, but inspection of Table 1 indicates that variations between samples and experiments obscure any such effects. We have performed the reduced parameter set fitting for A_1 equal to 1.4, 1.5, and 1.6 eV to reflect the small variations in activation energy for the low-temperature data sets and to indicate the dependence of the other parameters on the chosen A_1. Pending further work, we give less weight to the larger activation energy of the lherzolite because of the small temperature range of the measurements and the unknown complicating effects of secondary minerals in this rock. Our preferred value for A_1 is 1.6 eV, a prejudice based on the extended temperature range and data quality of the JCD experiment. Although there is less reason to believe that A_2 is identical for the three directions, we shall see that our ability to resolve this parameter is very poor, and so we keep the parameterization as simple as possible.

We fit the following model to data from all three axes of SCO: A_1, a low-temperature activation energy for all three axes; A_2, a high-temperature activation energy for all three axes; σ_{1a}, σ_{2a}, low- and high-temperature coefficients for [100]; σ_{1b}, σ_{2b}, low- and high-temperature coefficients for [010]; and σ_{1c}, σ_{2c}, low- and high-temperature coefficients for [001]. Results are tabulated in Table 2 and the response for A_1 = 1.6 eV is shown in Figure 2. Fixing the activation energies also has the advantage that the average conductivity model is estimated from all three data sets simultaneously, rather than estimating SO1 (which has a single A_1 also) from three independent fits.

The reduced number of parameters (7 free parameters compared with Shankland and Duba's 12) produces a slightly worse fit, but the misfit is still reasonable for these data. In fact, the removal of the 10 [010] points allows us to fit the conductivities better than Shankland and Duba for an A_1 of 1.1 eV. However, because the misfit applies to the high-temperature data only, it does not reflect our requirement that the low-temperature extrapolation fit the slope of the polycrystal data. That is, we are including outside constraints when fitting this data set, rather than taking a simple least squares fit for all parameters.

Our higher-temperature activation energies of 3.56–4.23 eV are comparable to 3.90 eV for SO1 and 3.33 eV of *Tyburczy and Roberts* [1990]. However, imposition of a uniform low-temperature activation energy results in values for the individual coefficients that differ from those obtained by *Shankland and Duba* [1990], even though the fit to the data is not very different, because of the high correlation among the fitting parameters, mentioned above. The three σ_{1i} in the new model, which have been forced to follow the observed anisotropy in the data at these temperatures, vary by a factor of about 2, while Shankland and Duba's original values varied by a factor of 50.

The correlation matrix for the A_1 = 1.6 eV model is

	σ_{1a}	σ_{1b}	σ_{1c}	σ_{2a}	σ_{2b}	σ_{2c}	A_2
σ_{1a}	1.00						
σ_{1b}	0.02	1.00					
σ_{1c}	0.11	0.16	1.00				
σ_{2a}	0.09	0.18	0.82	1.00			
σ_{2b}	0.13	0.03	0.84	0.94	1.00		
σ_{2c}	0.13	0.19	0.85	0.96	0.98	1.00	
A_2	0.13	0.19	0.86	0.96	0.98	1.00	1.00

(the logarithms of conductivity are implied here).

Fixing A_1 has, of course, removed what would otherwise be a strong correlation between that parameter and almost all others. Inspection of the residuals suggests that there are perhaps of the order of 10–20 degrees of freedom for this model, implying that a correlation coefficient above about 0.5 is sig-

TABLE 2. Parametric Fits to Conductivity–Temperature Data

Parameter	A_1=1.4	A_1=1.5	A_1=1.6 eV
$log_{10}(\sigma_{1a}$ S/m)	1.672	2.011	2.345 ± 0.003
$log_{10}(\sigma_{1b}$ S/m)	1.613	1.956	2.291 ± 0.003
$log_{10}(\sigma_{1c}$ S/m)	1.871	2.225	2.571 ± 0.004
$log_{10}(\sigma_{2a}$ S/m)	7.46	8.22	8.68 ± 0.51
$log_{10}(\sigma_{2b}$ S/m)	7.48	8.26	8.86 ± 0.50
$log_{10}(\sigma_{2c}$ S/m)	8.14	9.05	9.97 ± 0.49
A_2, eV	3.56	3.90	4.25 ± 0.17
RMS misfit	1.52%	2.00%	2.69%
$log_{10}(\bar{\sigma}_1$ S/m)	1.719	2.064	2.402
$log_{10}(\bar{\sigma}_2$ S/m)	7.69	8.51	9.17

Values for least squares fits to SCO data constrained by various values for A_1. The errors only apply for A_1 = 1.6 eV, but are similar for the other fits.

nificant. The first three eigenparameters are $\log(\sigma_{1a})$, $\log(\sigma_{1b})$, and $\log(\sigma_{1c})$ unmixed with other parameters, while the fourth is A_2 mixed partially with $\log(\sigma_{1c})$ and less with $\log(\sigma_{2c})$. The $\log(\sigma_{2i})$ are in unresolved eigenparameters and mixed together. Thus, if we accept 1.60 eV as a good value for A_1 then the errors given in Table 2 for the σ_{1i} are fairly reliable, the error for A_2 approximate and the errors on the σ_{2i} unreliable.

It is instructive to present the two components $\sigma_1 e^{-A_1/kT}$ and $\sigma_2 e^{-A_2/kT}$ of the fits graphically (Figure 2), which demonstrates several things. First, conductivity across the entire experimental range is dominated by the low-temperature $\sigma_1 e^{-A_1/kT}$. Second, the pattern of [001] being very much more conductive than [100] and [010] is maintained by the high-temperature mechanism. The reversed ordering of [100] and [010] in the high-temperature mechanism is not significant, as may be seen by the errors presented in Table 2, the lack of independence indicated by the correlation matrix, and its absence in the Shankland and Duba fits. Third, the higher-temperature mechanism exhibits more anisotropy than the lower-temperature mechanism. Similar examination of the individual fits presented by Shankland and Duba indicates that anisotropy exists even if the activation energies are not fixed and the [010] data are not truncated.

A MODEL FOR ISOTROPIC OLIVINE

Shankland and Duba [1990] demonstrated that with the exception of the parallel and series bounds (which are not isotropic), all the other mixing laws considered gave similar results, to within about 3%. The geometric mean has the advantage that it averages the three axes directly; the other mixing laws considered by Shankland and Duba are binary mixing laws that need to be applied to the parallel and series bounds. The geometric mean has the additional advantage that in this case, because of the fixed activation energy for the three axes, it preserves the underlying physical model for high and low temperature extrapolations. For example, for the low temperature extrapolation the geometric mean is given by

$$(\sigma_{1a}e^{-A_1/kT}.\sigma_{1b}e^{-A_1/kT}.\sigma_{1c}e^{-A_1/kT})^{1/3}$$

$$= (\sigma_{1a}.\sigma_{1b}.\sigma_{1c})^{1/3}e^{-A_1/kT}.$$

Geometric means for $\bar{\sigma}_1 = (\sigma_{1a}.\sigma_{1b}.\sigma_{1c})^{1/3}$ and $\bar{\sigma}_2 = (\sigma_{2a}.\sigma_{2b}.\sigma_{2c})^{1/3}$ are given in Table 2. Substitution of A_1, A_2, and these mean coefficients into (1) provides a simple expression for the average conductivity of isotropic olivine. This expression is accurate for temperatures of either A_1 or A_2 domination but will be in error in the transition region. The full expression for the geometric average is

$$\begin{aligned}\bar{\sigma} = [&\sigma_{1a}\sigma_{1b}\sigma_{1c}e^{-3A_1/kT} \\ &+ (\sigma_{1a}\sigma_{2b}\sigma_{1c} + \sigma_{2a}\sigma_{1b}\sigma_{1c} + \sigma_{1a}\sigma_{1b}\sigma_{2c})e^{-(2A_1+A_2)/kT} \\ &+ (\sigma_{2a}\sigma_{2b}\sigma_{1c} + \sigma_{1a}\sigma_{2b}\sigma_{2c} + \sigma_{2a}\sigma_{1b}\sigma_{2c})e^{-(A_1+2A_2)/kT} \\ &+ \sigma_{2a}\sigma_{2b}\sigma_{2c}e^{-3A_2/kT}]^{1/3}.\end{aligned}$$

The difference between the exact and approximate expressions is, however, much smaller than other uncertainties associated with our fitting procedure. It can be seen that the lower temperature fit $\bar{\sigma}_1$ is adequate for most geophysically relevant temperatures; significant curvature is not present up to about 1400°C ($1/T < 5.89 \times 10^{-4}$).

The new lherzolite data agree well with our prediction and support our choice of an activation energy of 1.6 eV. Although the activation energy fit to the lherzolite data (1.92 eV) is significantly higher than this, departure of the data from the model is very small, 0.05 decade at worst. The lherzolite data span only 1.5×10^{-4} 1/K, and given the complexity of the rock, it is inappropriate to extrapolate its behavior to 1500°C, so the single-crystal SCO data are still our best estimates of mantle material at high temperature. However, our ability to fit the conductivity of the lherzolite provides some vindication of our approach of constraining the low temperature behavior of the model.

ANISOTROPY AND CRYSTAL STRUCTURE

When activation energies are the same for all three directions, the relative magnitudes of the coefficients σ_{1i} then contain the measure of anisotropy, which we would like to relate to crystal structure. Normalizing to the [100] direction yields the conductivity ratios $\sigma_{1a}/\sigma_{1a} : \sigma_{1b}/\sigma_{1a} : \sigma_{1c}/\sigma_{1a}$, which when evaluated are 1.000 : 0.883 : 1.683. These ratios are virtually independent of the choice of A_1 and simply reflect the anisotropy that may be observed in the data. The dominant conduction mechanism inferred by *Schock et al.* [1989] in the better determined, low-temperature regime that we discuss here is the "small polaron" Fe^{3+} (= $Fe^{\bullet}_{Mg}$ in Kröger-Vink notation) produced by oxidation of Fe^{2+} (= $Fe^{\times}_{Mg}$). The problem of analyzing anisotropy for an electronic mechanism differs from that of ionic transport in which cations or their vacancies must move past the hexagonal close packed oxygen sublattice [e.g., *Condit*, 1985]. Another consideration for the polaron mechanism is the fact that only about 1 out of 11 Mg sites contain $Fe^{\times}$, and of these only a small fraction are $Fe^{\bullet}$.

Support for the polaron mechanism is provided by the positive thermoelectric coefficient below 1390°C [*Schock et al.*, 1989], dielectric measurements [*Sato*, 1986], and the increase of σ with iron content [*Hinze et al.*, 1982; *Hirsch et al.*, 1989; *Constable and Duba*, 1990]. Support is also provided by the positive dependence of conductivity on oxygen fugacity [*Schock et al.*, 1989; *Constable and Duba*, 1990]. Changing the oxidation state of Fe does not require migration of oxygen defects. As noted by Schock et al., reequilibration of conductivity after a change in f_{O_2} is accomplished on time scales of 10^3 s, much too rapid for the diffusion of oxygen into the samples, which occurs on time scales of 10^7 s. Several other physical and chemical changes are also observed to reequilibrate with changes in f_{O_2} on similar time scales [e.g. *Boland and Duba*, 1985; *Mackwell et al.*, 1988; *Kohlstedt and Vander Sande*, 1975], but the most direct evidence that the oxidation state (rather than some other property) of the interior of olivine grains can be rapidly influenced by changes in external f_{O_2} is presented by *Pasteris and Wanamaker* [1988], who produced CO and graphite in CO_2 inclusions in SCO on time scales a short as 1 hour after changing the f_{O_2} of the experimental atmosphere. Metal ion vacancies [*Pasteris and Wanamaker*, 1988] and electronic transport [*Boland and Duba*, 1985] have both been suggested as mechanisms by which the internal oxidation state of olivine is rapidly changed.

Taking the unit cell size for Fo_{91} to be a linear interpolation between forsterite and fayalite, or $a = 4.759 \times 10^{-10}$ m, $b = 10.216 \times 10^{-10}$ m, $c = 5.988 \times 10^{-10}$ m, shows that nearest-neighbor Mg sites most closely aligned along the three principal directions are fairly equally spaced: $\sqrt{[(a/2)^2 + (b/4)^2 + (c/4)^2]} : \sqrt{[(a/2)^2 + (b/4)^2]}$ (short hop) or $\sqrt{[(a/2)^2 + (b/4)^2 + (c/4)^2]}$ (long hop) : $c/2$, which can

be normalized to the ratios 1.000 : 0.919 (or 1.000 for long hop) : 0.788. The relation between diffusion and hopping mobility [e.g., *Honig*, 1966] predicts that conductivity should be proportional to the square of the hopping distance, which in this case would give the ratios 1.000 : 0.845 (or 1.000) : 0.621. However, none of these ratios are in the order of the conductivity anisotropy ratios given above.

A hypothesis that accounts for the conductivity anisotropy ratios comes from observing that the olivine structure contains two different crystallographic sites that Mg and Fe can occupy, M1 and M2. $Fe^{\bullet}$ is a smaller ion than $Fe^{\times}$, and if it prefers the smaller M1 site, then the hopping distances would be the M1–M1 distances closest to the three principal axes. Their ratios are $a : \sqrt{[(a/2)^2+(b/2)^2]} : c/2$ or 1.000 : 1.184 : 0.629. More significantly, reciprocals of these ratios are 1.000 : 0.845 : 1.590; the latter are not only in the proper order for the conductivity anisotropy ratios but match them to within about 5%. The inference from this agreement is intuitively favorable, namely, that hopping probability is inversely proportional to hopping distance. Such a dependence is often given as a qualitative explanation of conductivity anisotropy [*Schock et al.*, 1989; *Ottonello et al.*, 1990] despite the presumed dependence on the square of the hopping distance. We see then that placing all the low-temperature anisotropy in the σ_1 term by fixing A_1 permits hypothesizing both a crystallographic ordering of $Fe^{\bullet}$ and a polaron hopping parameterization.

Crystallographic studies have somewhat ambiguous implications for this picture. Experiments [*Aikawa et al.*, 1985; *Ottonello et al.*, 1990] and theory [*Ottonello et al.*, 1990] indicate a moderate preference of $Fe^{\times}_{Mg}$ for the M1 site, principally an effect of crystal field stabilization. This distribution increases with temperature, but may not be substantial enough to account for the low-temperature anisotropy in σ_{1i}. A more difficult problem comes from theoretical models [*Ottonello et al.*, 1990] that imply $Fe^{\bullet}_{Mg}$ should be strongly stabilized on M2. (For comparison, M2-M2 shortest distances are $\sqrt{[(a/2)^2 + (c/2)^2]} : \sqrt{[(a/2)^2 + (b/2)^2]} : \sqrt{[(a/2)^2 + (c/2)^2]}$, which yield the ratios 1.000 : 1.473 : 1.000, again in the wrong order.) Another issue that cannot presently be addressed is that of second nearest-neighbor hopping when nearest-neighbor sites are too few to interact.

The variation in coefficients for the high-temperature conduction mechanism is much larger, having an order of magnitude variation between the most conductive [001] direction and the other two. The strong variation adds to the arguments of *Schock et al.* [1989] for an ionic mechanism (magnesium vacancies) at high temperature; thus the considerations discussed by *Condit* [1985] for ionic diffusion are relevant to the interpretation of anisotropy. *Ottonello et al.* [1990] argue that the anistropy is enhanced by a preference of V''_{Mg} for M1 whose shortest jump distances are along [100]. It is interesting that for the ionic case the ordering of conductivity anisotropy, although not the quantitative values, is again of the order of the reciprocals of jump distances, which are in this case the nearest-neighbor distances above. However, in view of untreated geometrical factors (the jump vectors are not parallel to the principal axes) and the errors and strong covariances in the high temperature σ_{2i}, it would be reckless to attempt a quantitative interpretation. The strong anisotropy for the high-temperature mechanism is consistent with its being ionic (Mg vacancies) and the low-temperature mechanism being electronic (polarons) as hypothesised by *Hughes* [1955], *Sato* [1986], and *Schock et al.* [1989].

SUMMARY AND CONCLUSIONS

Because high-temperature conductivity measurements are difficult to make on polycrystalline material, the most reliable measurements above 1100°C have been made on single-crystal specimens. Olivine conductivity is anisotropic, and so the conductivity in the three crystal directions must be averaged in some way if an estimate of conductivity for an isotropic olivine mantle is desired. The geometric mean of the parametric fit to the three-axis data is, to good approximation, given by $\bar{\sigma} = 10^{2.402}e^{-1.60eV/kT} + 10^{9.17}e^{-4.25eV/kT}$. Between 720°C and 1500°C, uncertainties in this model are likely to be less than those discussed by *Shankland and Duba* [1990] and, in principle, provide a means of obtaining temperature from conductivity under lithospheric (subsolidus) conditions. Alternatively, if one has a thermal model for the lithosphere, conductivities can be predicted and compared with field data, as done by *Heinson and Constable* [1991].

The accepted model for electrical conduction in silicate minerals by means of thermally activated point defects is described by the sum $\sum \sigma_i e^{-A_i/kT}$ (k is Boltzmann's constant and T absolute temperature). σ_i and A_i are a coefficient and activation energy particular to conduction mechanism i. A conclusion from electrical conductivity versus temperature data from both single-crystal and polycrystal olivines is that below about 1400°C one activation energy is satisfactory for all three crystallographic axes. The strong correlation between activation energies and coefficients makes it difficult to reach this conclusion by examination of three-axis, high-temperature (1200°–1500°C) data independently of lower-temperature data. The dominant activation energy for temperatures between 720° and 1500°C is about 1.6 eV, in accordance with the relatively low temperature experiments of *Duba et al.* [1974], *Constable and Duba* [1990], and *Tyburczy and Roberts* [1990]. Parametric fits to high-temperature single crystal data of *Shankland and Duba* [1990] in which the low temperature activation energy is held constant at this value yield precise estimates of the preexponential coefficients in each crystallographic direction, with little covariance between parameters. It is observed that anisotropy in conduction, as represented by the ratios of these coefficents, is the same as the interionic distances for the M1 magnesium sites, implying both that interionic spacing determines the efficiency of conduction and that Fe^{3+} substitutes preferentially at M1 sites at temperatures above 1200°C.

Acknowledgments. The authors thank Lee Hirsch and two anonymous reviewers for comments on the manuscript. Part of this work was conducted while SC was a visiting scholar at the Australian National University; he wishes to thank the University for that support and also Ian Jackson for many discussions during that stay. This work was supported by the Los Alamos branch of the Institute of Geophysics and Planetary Physics and by the Office of Basic Energy Sciences of the Department Energy under contract with 7405-ENG-36 (LANL) and 7405-ENG-48 (LLNL).

REFERENCES

Aikawa, N., M. Kumazawa, and M. Tokonami, Temperature dependence of intersite distribution of Mg and Fe in olivine and the associated change of lattice parameters, *Phys. Chem. Miner.*, *12*, 1–8, 1985.

Bevington, P.R., Data Reduction and Error Analysis for the Physical Sciences, McGraw-Hill, New York, 1969.

Boland, J.N., and A.G. Duba, An electron microscope study of the stability field and degree of nonstoichiometry in olivine, *J. Geophys. Res.*, *91*, 4711–4722, 1986.

Condit, R.H., An approach to analysing diffusion in olivine, in *Point*

Defects in Minerals, Geophys. Monogr. Ser., vol. 31, edited by R. N. Schock, pp. 106–115, AGU, Washington, D.C., 1985.

Constable, S.C., and A. Duba, Electrical conductivity of olivine, a dunite and the mantle, *J. Geophys. Res.*, *95*, 6967–6978, 1990.

Crow, E.L., F.A. Davis and M.W. Maxfield, Statistics Manual, Dover, New York, 1960.

Duba, A., H.C. Heard, and R.N. Schock, Electrical conductivity of olivine at high pressure and under controlled oxygen fugacity, *J. Geophys. Res.*, *79*, 1667–1673, 1974.

Duba, A.G., R.N. Schock, E. Arnold, and T.J. Shankland, An apparatus for measurement of electrical conductivity to 1500°C at known oxygen fugacity, in *The Brittle-Ductile Transitions in Rocks, The Heard Volume, Geophys. Monogr. Ser.*, vol. 56, edited by A.G. Duba, W.B. Durham, J.W. Handin and H.F. Wang, pp. 207–210, AGU, Washington, D.C., 1990.

Heinson, G. and S. Constable, The electrical conductivity of oceanic upper mantle, *Geophys. J. Int.*, in press, 1991.

Hinze, E., G. Will, L. Cemiĉ, and M. Manko, Electrical conductivity measurements on synthetic olivines at high pressures and temperatures under defined thermodynamic conditions, in *High-Pressure Researches in Geoscience*, edited by W. Schreyer, pp. 393–406, E. Schweizerbart'sche, Stuttgart, 1982.

Hirsch, L.M., T.J. Shankland, and A. G. Duba, Electrical conductivity and mobility in olivine (abstract), *EoS Trans. AGU*, *70*, 1369, 1989.

Honig, J.M., Electrical properties of metal oxides which have "hopping" charge carriers, *J. Chem. Educ.*, *43*, 76–82, 1966.

Hughes, H., The pressure effect on the electrical conductivity of peridot, *J. Geophys. Res.*, *60*, 187–191, 1955.

Jupp, D.L.B., and K. Vozoff, Stable iterative methods for the inversion of geophysical data, *Geophys. J.R. Astron. Soc.*, *42*, 957-975, 1975.

Kohlstedt, D.L., and J.B. Vander Sande, An electron microscopy study of naturally occurring oxidation-produced precipitates in iron-bearing olivines, *Contrib. Miner. Petrol.*, *53*, 13–24, 1975.

Lanczos, C., Linear Differential Operators, D. Van Nostrand, Princeton, N.J., 1960.

Mackwell, S.J., D. Dimos, and D.L. Kohlstedt, Transient creep of olivine: Point-defect relaxation times, *Phil. Mag. A*, *57*, 779–789, 1988.

Marquardt, D.W., An algorithm for least-squares estimation of nonlinear parameters, *J. Soc. Ind. Appl. Math.*, *11*(2), 431-441, 1963.

Ottonello, G., F. Princevalle, and A. Della Giusta, Temperature, composition, and f_{O_2} effects on intersite distribution of Mg and Fe^{2+} in olivines, *Phys. Chem. Miner.*, *17*, 301–312, 1990.

Pasteris, J.D., and B.J. Wanamaker, Laser Raman microprobe analysis of experimentally re-equilibrated fluid inclusions in olivine: Some implications for mantle fluids, *Amer. Miner.*, *73*, 1074–1088, 1988.

Sato, H., High temperature a.c. electrical properties of olivine single crystal with varying oxygen partial pressure: Implications for the point defect chemistry, *Phys. Earth Planet. Inter.*, *41*, 269–282, 1986.

Schock, R.N., A. Duba, and T.J. Shankland, Electrical conduction in olivine, *J. Geophys. Res.*, *94*, 5829-5839, 1989.

Shankland, T.J., and A.G Duba, Standard electrical conductivity of isotropic, homogeneous olivine in the temperature range 1100-1500°C, *Geophys. J. Int*, *103*, 25–31, 1990.

Tyburczy, J.A., and J.J. Roberts, Low frequency electrical response of polycrystalline olivine compacts: Grain boundary transport, *Geophys. Res. Lett.*, *17*, 1985–1988, 1990.

S. Constable, Institute of Geophyscis and Planetary Physics, 0225, Scripps Institution of Oceanography, La Jolla, CA 92093-0225.

A. Duba, Lawrence Livermore National Laboratory, L201, Livermore, CA 94550.

T.J. Shankland, Los Alamos National Laboratory, MS C335, Geophysics Group, Los Alamos, NM 87545.

**(Received January 11, 1991;
revised August 26, 1991;
accepted September 18, 1991.)**